Hindawi Publishing Corporation
International Journal of Photoenergy
Volume 2012, Article ID 637943, 7 pages
doi:10.1155/2012/637943

Research Article

Optimised In_2S_3 Thin Films Deposited by Spray Pyrolysis

Hristina Spasevska,[1] Catherine C. Kitts,[2,3] Cosimo Ancora,[2] and Giampiero Ruani[2]

[1] *Faculty of Electrical Engineering and Information Technologies, Ss. Cyril and Methodius University, 1000 Skopje, Macedonia*
[2] *Consiglio Nazionale delle Ricerche (CNR), Istituto per lo Studio dei Materiali Nanostrutturati (ISMN), Via P. Gobetti 101, 40129 Bologna, Italy*
[3] *Department of Physical Chemistry, Chalmers University of Technology, Kemivagen 10, 41296 Gothenburg, Sweden*

Correspondence should be addressed to Hristina Spasevska, hristina@feit.ukim.edu.mk

Received 29 September 2011; Accepted 28 October 2011

Academic Editor: Yuexiang Li

Indium sulphide has been extensively investigated as a component for different kind of photovoltaic devices (organic-inorganic hybrid devices, all inorganic, dye sensitized cells). In this paper, we have optimised the growth conditions of indium sulphide thin films by means of a low cost, versatile deposition technique, like spray pyrolysis. The quality of the deposited films has been characterised by micro-Raman, vis-UV spectroscopy, and atomic force microscopy. Substrate deposition temperature and different postdeposition annealing conditions have been investigated in order to obtain information about the quality of the obtained compound (which crystalline or amorphous phases are present) and the morphology of the deposited films. We have shown that the deposition temperature influences strongly the amount of amorphous phase and the roughness of the indium sulphide films. Optimised postdeposition annealing treatments can strongly improve the final amount of the beta phase almost independently from the percentage of the amorphous phase present in the as deposited films.

1. Introduction

In recent years, indium sulphide (In_2S_3) has become a prominent wide bandgap semiconductor, used for low-cost three-dimensional mesoporous nanostructured solar cells based on n-type TiO_2 and p-type $CuInS_2$ (CIS) as a buffer layer [1, 2] or directly as a dye in an electrochemical dye-sensitized solar cells [3] as well as a solar radiation activated photocatalyser [4, 5]. Both these applications are based on the exploitation of solar radiation; the former to produce energy, the latter to degrade organic pollutant. Solar energy, and in particular photovoltaics (PV) which directly converts photons in electrons, represents one of the most relevant and direct renewable and clean energy sources that can successfully replace fossil fuels (oil, gas, coal) in view of their finite nature. This, together with the increasing environmental concern of the irreversibility of climate changes that can be induced by anthropic activity, has contributed to the larger attention both of individuals and institutions towards the development of low-cost and short pay-back energy photovoltaic systems. In fact, at the moment, a large-scale application of conventional PVs is mainly limited by two factors: the energetic costs needed to produce, install, and dispose PV cells and modules based on Si technologies, and the still too high noncompetitive economic costs. Nevertheless, the PV global market has shown an almost constant growth of about 40% each year during last decade. Three-dimensional structured PV devices, like bulk all organic (see ref. [6] and references therein), hybrid hetero-junctions (see ref. [7] and refs. therein), or dye sensitized solar cells [8], represent a real low-cost short-energy payback time, which is an alternative to the currently dominant Si technologies. Grätzel research group [8] has shown that nanostructured based solar cell can reach relatively high performances (certified conversion efficiency of sunlight into electricity of 10.4% [9]) using not extremely sophisticated technological approaches as in the case of silicon electronic industry. These devices were named Dye Sensitized Solar Cells (DSSCs) or Grätzel cells, from the name of the inventor. The DSSCs are constituted

by a sensitizer (dye) adsorbed on a porous semiconducting oxide film; photoexcitation of the dye induces the injection of an electron into the conduction band of the oxide. The photogenerated electrons diffuse through the porous semiconducting film to the electrode and then through the external circuit to the counter electrode. The dye is then neutralized by the electron donation from the electrolyte that is regenerated at the counter electrode.

Such an approach generated a large research activity in maintaining the same approach but following different pathways: implementing the characteristics of the liquid electrolyte-based devices, substituting it with a solid-state hole conductor [10, 11], or substituting both the metal-organic dye and the electrolyte with an inorganic semiconductor like CIS [12].

In the latter case, it was shown that the introduction of an indium sulphide buffer layer in between the two semiconductors in all-inorganic dye cells improves the performances of the devices. The In_2S_3 buffer layer, between the n-type and p-type regions, contributes to the junction rectification and to the reduction of the possibilities of recombination/annihilation of the photogenerated charge carriers at the TiO_2/CIS interface [12]. It was shown that, as buffer layer, In_2S_3 can be also be used as an alternative to CdS in CIS thin films solar cells to develop efficient Cd-free device [13].

Spray pyrolysis has been used since 1982, as a possible low-cost deposition technique in photovoltaics [14]. In case of TiO_2/CIS photovoltaic cells, spray pyrolysis is used as deposition technique for the buffer In_2S_3, the active CIS layers [15], as well as the thin compact TiO_2 layer. The introduction of this low-cost deposition technique in photovoltaic technology could result in a revolution for PV industrial field, allowing the production of photovoltaic devices in large scale with relatively low-cost, simple technologies. This technology can be easily integrated in industrial processes like those used in glass and ceramic industries; large-scale facilities for coating on glass of F:SnO_x have already been developed [16] and can be easily extended to the deposition of different semiconductors.

Depending upon growth temperature and pressure, In_2S_3 exists in three crystallographic forms: α, β, and γ. Tetragonal β-In_2S_3 is the most stable form at room temperature and also the more suitable to act as buffer layer between TiO_2 and CIS in the fabrication of PV devices. As a consequence, after the deposition process, the In_2S_3 film is exposed to thermal cycles either as dedicated annealing treatments to improve the buffer layer quality or as consequence of the sequential deposition of other layers like CIS and the final counter electrode.

Several authors have pointed their attention to improve the quality of the In_2S_3 films by varying the deposition condition and postdeposition treatments [2, 17]. In this paper, the structural and optical properties of single films, as a function of the deposition condition, are investigated in order to determine the optimised parameters in order to maximize the efficiency of the final device. In particular, we investigated the deposition and postdeposition treatment parameters of the In_2S_3 buffer layer to be used in TiO_2/CIS nanocomposite solar cells. Spectroscopical and morphological properties of In_2S_3 films are analyzed.

2. Experimental

In_2S_3 films are deposited by spray pyrolysis on three different substrates (glass, glass/SnO_2 : F, and glass/SnO_2 : F/TiO_2) with temperatures ranging from 220°C to 340°C.

The precursor solution, used in this set of experiments, contains $InCl_3$ (99.999%) and thiourea (99%) dissolved in water (In : S = 1 : 7) and is delivered to the nozzle with 1 mL/min flow rate (the high sulphur, indium ratio was selected in accordance with the findings of John et al. [18]). In order to prevent any possible degradation of the solutions, we always worked with fresh solutions prepared immediately before been sprayed. A Sonaer 130K50T ultrasonic atomized nozzle, driven by Sonaer digital ultrasonic generator working at 130 KHz, was used for spraying the solution on the hot substrate. The amplitude of the oscillations is tuned in order to obtain the best atomization of the sprayed solution. An N_2 flow (10 l/min) is used as carrier gas to direct the atomized solution toward the substrate. The distance between the nozzle and the substrate is set at 20 cm and the deposition temperature (T_{dep}) is controlled by a thermocouple placed close to the edge of the substrate and connected to a digital electronic temperature controller TLK 48. The temperature on the surface of the substrate was measured by an infrared thermometer Fluke 572, the temperatures measured at the surface of the substrate were systematically between 5 and 8 degree lower than those measured by the thermocouple; the temperatures reported in this paper are those measured by the infrared thermometer. In order to maintain the temperature of the substrate constant during the deposition, the nitrogen flow was switched on two minutes in advance with respect to the injection of the liquid into the nozzle letting the system to equilibrate. All the investigated films have been obtained spraying 4 mL of precursor solution (with a spray rate of 1 mL/min) obtaining a final thickness of about 100 nm, the thickness of the various films was measured by profilometry. We spray deposited onto two substrates at the same time ($10 \times 10\,mm^2$) obtaining homogeneous films thanks to the geometry of the carrying gas flux.

After a first characterization, the deposited samples were annealed in air at temperatures ranging from 400°C up to 500°C; the annealing was carried out warming the oven at a rate of 100° per hour up to the desired temperature, and after one hour of annealing, the temperature was then decreased at the same rate. Some of the pristine films have been treated by rapid thermal annealing (RTA) at 500°C in air by using a home-made halogen lamps RTA-based setup.

All the samples have been characterised spectroscopically and morphologically in air at room temperature.

Confocal micro-Raman spectra were recorded in the unpolarized backscattering geometry through a Renishaw 1000 system using the 514.5 nm (2.41 eV) Ar+ laser line focused on the sample through a ×100 objective lens and a laser spot of approximately 1 μm. The laser power used

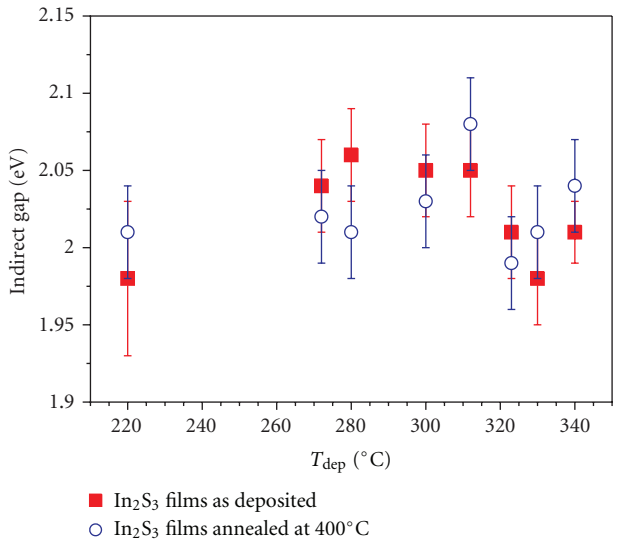

Figure 1: Energy of the indirect gap extrapolated from optical conductivity measurements (1) on In_2S_3 films on glass, as deposited (red open squares) and after annealing in the furnace at 400°C (blue open circles).

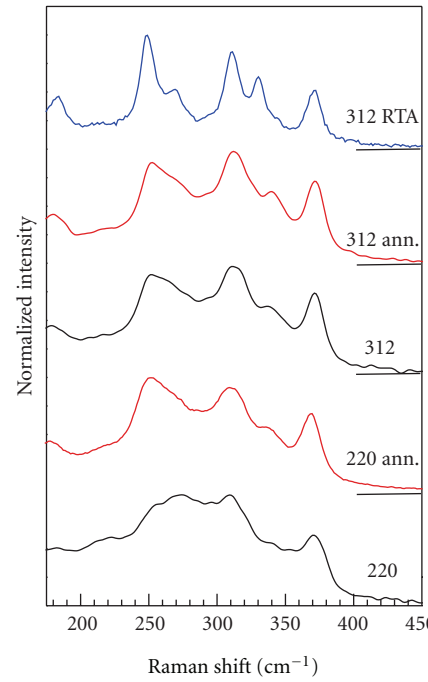

Figure 2: Raman spectra of In_2S_3 films deposited at 220°C and 312°C (220, 312, resp.): black lines. Raman spectra of the same films after one hour annealing at 500°C in the furnace (220 ann, 312 ann): red lines. Raman spectrum of In_2S_3 films deposited at 312°C after 1 min. rapid thermal annealing at 500°C (312 RTA): blue line.

was in the range of 80–150 μW (power density range of 1-2 KW/cm^2). In order to obtain a good signal-to-noise ratio, the spectrum acquisition time was typically 20 min. The spectrometer resolution is about 4 cm^{-1} for the laser line used.

NIR-VIS absorption measurements have been performed by using a double-beam spectrophotometer (JASCO V500) in the spectral region from 1.4 eV to 3.6 eV.

Atomic force microscopy (AFM) images were collected using an NT-MDT Solver Scanning Probe Microscope in tapping mode.

3. Results and Discussion

In literature, there are conflicting theories about the semiconducting nature of β-In_2S_3 whether the system has a direct or indirect gap. According to us, the most recent and reliable paper on this item is the one published by Barreau et al. [19]. From experimental data and density functional theory calculation, they conclude that β-In_2S_3 has an indirect gap of 2.01 eV whose value is strongly correlated to the sulphur concentration [20]. Through absorbance measurements, it is possible to determine the bandgap energies of a semiconducting thin film. In fact, within the approximation of parabolic electronic bands for an indirect semiconductor, the absorption coefficient α is correlated to the bandgap energy (E_g) as follows:

$$\alpha(h\nu) \propto \frac{\left(h\nu - E_g\right)^2}{h\nu}. \quad (1)$$

Consequently, plotting $(\alpha h\nu)^{0.5}$ versus $h\nu$, the extrapolation at zero of the linear part of the curve gives the optical bandgap.

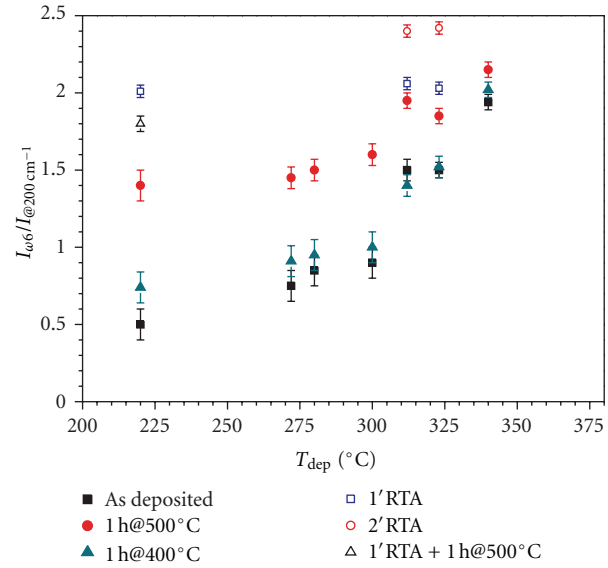

Figure 3: Deposition substrate temperature dependence of the relative intensity of the ω_6 phonon mode with respect to the background at 200 cm^{-1} of the Raman spectra In_2S_3 films as deposited (full squares) and after postdeposition annealing treatments. One hour annealing at 400°C in furnace (full triangles); one hour annealing at 500°C in furnace (full circles); one minute rapid thermal annealing at 500°C (open squares); two minutes rapid thermal annealing at 500°C (open squares); one minute rapid thermal annealing at 500°C followed by one hour annealing at 500°C in furnace (open triangles).

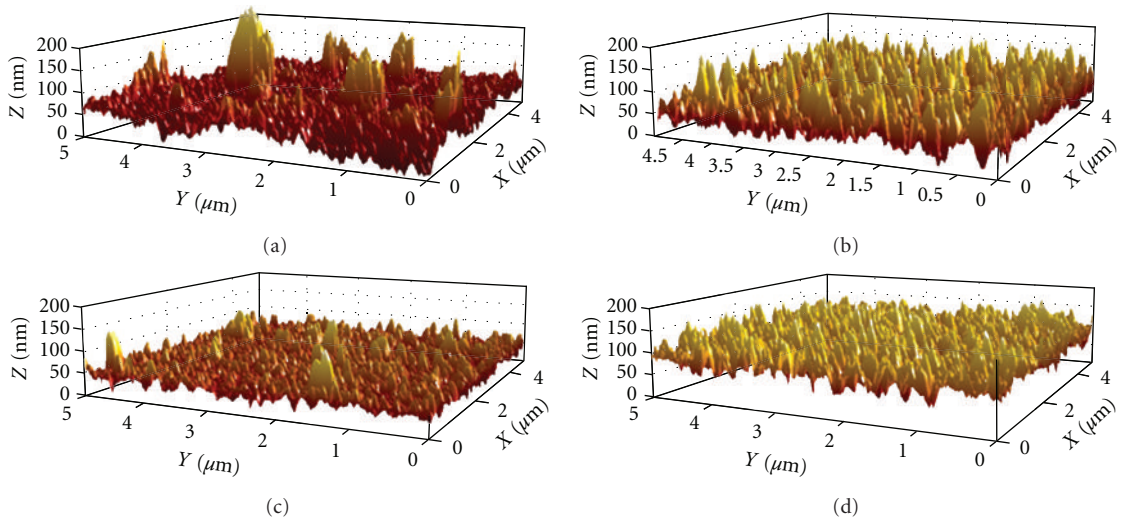

FIGURE 4: *3D* AFM images ($5 \times 5\,\mu m^2$) of as-grown films of In_2S_3 deposited at different substrate temperature (a) 272°C, (b) 300°C, (c) 323°C, and (d) 340°C.

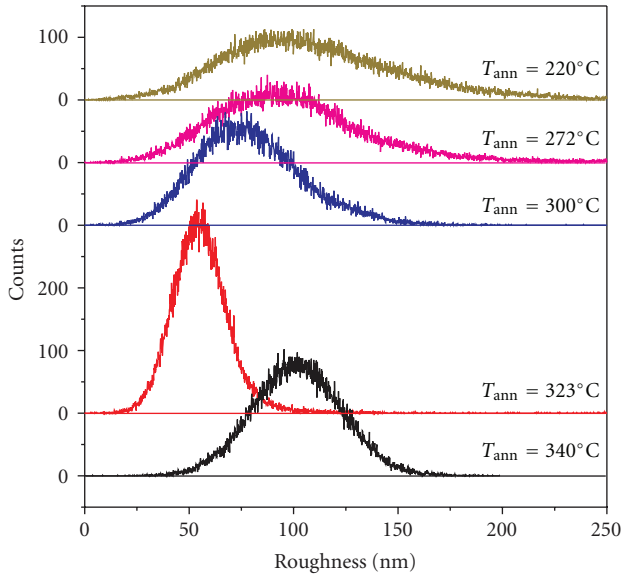

FIGURE 5: Height distribution histograms obtained by analysing $10 \times 10\,\mu m^2$ AFM images measured on In_2S_3 pristine films deposited at different temperatures.

In Figure 1, the values extrapolated from the $(\alpha h\nu)^{0.5}$ versus $h\nu$ plots are reported as a function of the deposition temperature. The reported data refer to the as-deposited In_2S_3 films on glass/SnO_2 : F/TiO_2 (open squares), and after annealing at 400°C (open circles), similar results have been obtained for films annealed also at 500°C. As a result, we have observed that all the analyzed films, independently of the substrate material, deposition temperature, and postannealing temperature (T_{ann}), show almost the same energy gap of about 2 eV. This value is comparable with the one of the In_2S_3 single crystal [21] and the one measured on films grown by atomic layer deposition [22]. As already mentioned, the value of the energy gap is strongly influenced by the stoichiometry [21] of the semiconductor, it is possible to argue that the In_2S_3 films obtained by spray pyrolysis are almost stoichiometric and that the annealing procedure, in the temperature range that we have investigated, do not alter the In/S ratio of the deposited films.

The Raman scattering strongly depends not only on the nature of the investigated system but also on the crystallographic form and crystallinity of the compound. Raman spectroscopy is a nondestructive and relatively fast experimental technique to determine the phase and the quality of the deposited films.

The Raman spectra reported in Figure 2 refer to films of In_2S_3 on glass grown at different deposition temperatures and/or annealing treatments. The Raman spectra show the presence of the β phase in all the films [23, 24]. The peak position and the half width of the β phase Raman bands show a dependence of the degree of crystallinity from the deposition and annealing treatments.

A featured background centred around 300 cm^{-1}, whose intensity strongly depends on deposition temperature, is also observed in almost all the spectra. This feature is strongly dependent on the thermal history of the film. The Raman spectra of In_2S_3 films deposited at low temperatures (220°C) are dominated by this broad structure; most of the phonon bands of In_2S_3 are very weak, the only clearly detectable feature is the one at about 370 cm^{-1} associated with the A_{1g} Raman mode (see ref. [24] and reference therein) identified now with ω_6. By increasing the deposition temperature, the Raman active phonon modes become more prominent and their intensities with respect to the background increase with increasing temperature; the F_{2g} at 180 cm^{-1} (ω_1), the A_{1g} at 250 cm^{-1} (ω_2), and the A_{1g} at 310 cm^{-1} (ω_4) modes are clearly observed while the E_g at 270 cm^{-1} (ω_3) and the F_{2g} at 330 cm^{-1} (ω_5) modes appear as shoulders. As one of the parameters used to measure the quality of the film, we

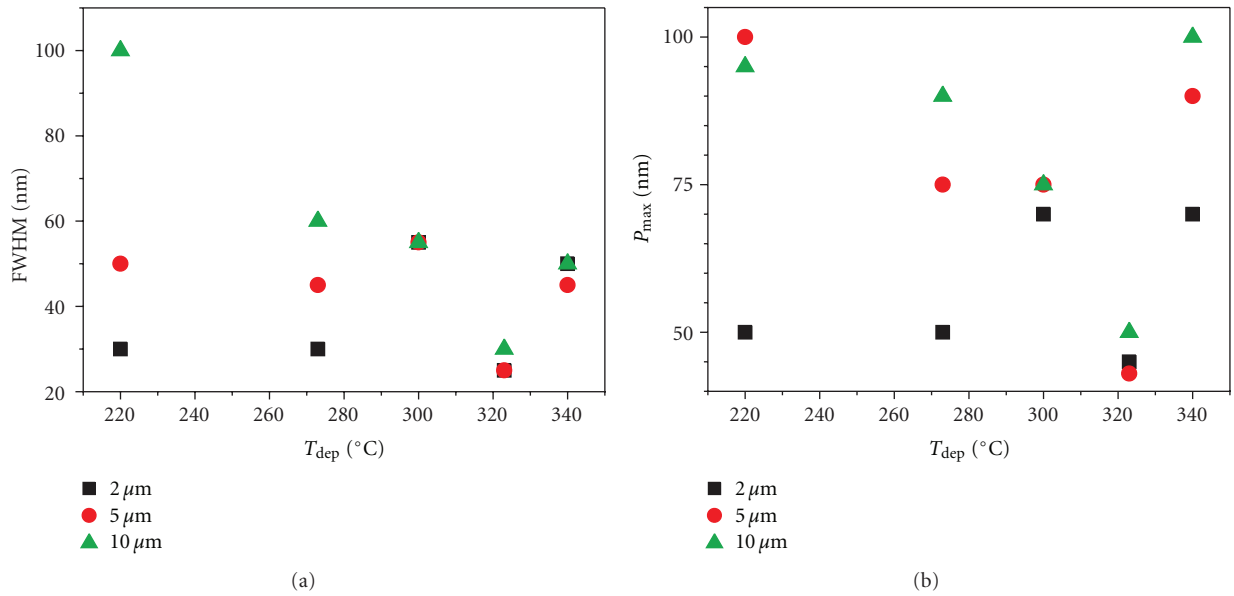

Figure 6: Deposition temperature dependence of height distribution parameters: (a) full widths at half maximum (FWHM) and (b) peak maximum (P_{max}) of In_2S_3 films evaluated on different scales ($2 \times 2\,\mu m^2$, $5 \times 5\,\mu m^2$, and $10 \times 10\,\mu m^2$).

plotted in Figure 3 the relative intensities of the ω_6 peak with respect to the background associated to the amorphous state versus the deposition temperature. We chose the ω_6 mode because it does not overlap with the background and it is clearly detected also in samples grown at low temperature.

The Raman spectra performed on annealed films show an improvement in the quality of the films (see Figure 2). The heat treatment at 400°C improves significantly only the films deposited at low temperature (220°C); up to 300°C, a moderate improvement of the film quality is observed while, at higher deposition temperature, the observed variations are within the error bars.

The annealing at higher temperature in the furnace, $T_{ann} = 500$°C, shows an overall improvement in the quality of the films (see Figure 2, red curves and Figure 3, full circles). The amount of the amorphous phase decreases significantly in all the annealed samples. The peak position and half widths of the Raman modes of In_2S_3, that can be related to the dimension of the crystallites, do not change significantly with the heat treatment, except in the case of films deposited at low temperature ($T_{dep} = 220$°C). This means that the dimensions of the crystallites are not influenced by the heat treatment.

In some of the pristine films, we also performed RTA heat treatment at 500°C with different annealing time (1 and 2 minutes). With respect to the heat treatment in the furnace, RTA-treated films show a further improvement (see Figures 2 and 3). The increase of the intensity of the active Raman modes with respect to the background similar to the ones obtained for films deposited at relatively high temperature (<300°C) and annealed in furnace at 500°C are obtained in all the films, independently from T_{dep}, after 1 min. RTA thermal treatment at 500°C shows a significant decrease in the amorphous component. Moreover, the half-widths of all the Raman peaks are strongly reduced in a way that the two modes indexed as ω_3 and ω_5 now appear clearly as peaks, well separated from the two more intense ω_2 and ω_4 modes. This is a clear index of an improvement of the crystallinity of the films. The Raman spectra obtained analysing films after a longer RTA thermal treatment at 500°C (2 min.) show that their quality is further improved. Moreover, the peak energies recorded for these samples coincide with those observed in β-In_2S_3 crystals [25].

As already mentioned, the In_2S_3 film within a PV device being used as buffer layer between the TiO_2 and CIS will be subject to the heat treatment necessary for the deposition and annealing of the CIS layer at temperature around 400°C or, in the case of deposition of a transparent counter electrode like conducting oxides, the film can be exposed also at higher temperature (up 500°C). In order to verify if further heat treatment will alter the improvement of the quality of the In_2S_3 film obtained by RTA, the sample deposited at 220°C and treated by RTA for 1 minute at 500°C was subsequently annealed for one hour in the furnace at 400°C. The Raman spectrum was not altered by this treatment. Only when the film was annealed in the furnace at 500°C, the peaks become slightly broader and consequently the relative height of the ω_6 mode with respect to the background decreases.

Morphological characterizations of the In_2S_3 films have been performed by AFM. The roughness of the deposited films shows a strong dependence with the deposition temperature while we did not find any detectable change at any heat treatments the film were exposed to in these set of experiments, showing that a mass transport if it occurs during annealing is limited to short-range diffusion. Films deposited at low temperature show a relatively large roughness characterized by asperities very dispersed in dimensions. By increasing the substrate deposition temperature, the

roughness and the size dispersion of the grains constituting the In_2S_3 films decrease continuously reaching a minimum around 320°C. At this temperature, the trend is inverted and the films deposited at higher temperature show again an increase in the roughness as a consequence of the formation of larger crystalline agglomerates (see Figures 4, 5, and 6).

4. Conclusions

The characterisation of films obtained by spray pyrolysis has shown a negligible dependence of the composition by the deposition temperature of the substrate and the post-deposition treatments like annealing at high temperature in the furnace and RTA. On the other hand, both morphology and crystallinity of In_2S_3 spray-deposited films are strongly influenced by their thermal history. The presence of an amorphous component in the films decreases by increasing the deposition temperature. The annealing at 400°C improves the quality of the films only in the case of films deposited at relatively low temperature ($T_{dep} < 300$°C). Except the films grown at $T_{dep} = 340$ (that are characterised by the presence of a small amorphous phase), all the other films annealed in furnace at higher temperature ($T_{ann} = 500$°C) show a relatively high improvement of their quality with a larger reduction of the amorphous component. The final quality of the In_2S_3 spray-deposited films exposed to RTA annealing at $T_{ann} = 500$°C does not depend on the deposition temperature, but from the annealing time, we have observed that after 1 minute of rapid thermal annealing all the Raman peaks become sharper and the background associated to the amorphous component strongly decreases. The films exposed for longer time (2 minutes) to RTA annealing show a further decrease of the amount of the amorphous phase. Additional heat treatments at temperature up to 400°C, temperatures at which the In_2S_3 films can be exposed when further layers of different components are deposited in the process of preparation of complex devices like TiO_2/CIS photovoltaic cells, will not alter the quality of the indium sulphide layer. On the other hand, the heat treatment at higher temperature ($T_{ann} = 500$°C) of the films annealed using RTA procedure shows a reduction of the crystallinity of the compound.

We have observed that the deposition temperature strongly affects the roughness of the In_2S_3 films, and the smoothest films are obtained at about 320°C.

The reduced roughness and the high-quality films of β-phase In_2S_3, deposited by spray pyrolysis at $T_{dep} = 320$°C and annealed in air by RTA for 2 minutes at $T_{ann} = 500$°C as well as the observation that further thermal cycles at which the film can be exposed with temperatures up to 400°C, show that this growth condition and postdeposition treatments are suitable for the deposition of In_2S_3 as buffer layer in between TiO_2 and CIS in the preparation of photovoltaic devices.

Acknowledgments

The authors thank Messrs Tiziano Bonfiglioli, Paolo Mei, Mauro Murgia, and Salvino Rose for valuable technical assistance. This research was supported by the Central European Initiative KEP Project (CHEAP-CELL), Progetto CNR EFoR and the Project "Deposition, characterization and parametric studies of nanostructured solar cells."

References

[1] R. O'Hayre, M. Nanu, J. Schoonman, and A. Goossens, "Mott - Schottky and charge-transport analysis of nanoporous titanium dioxide films in air," *Journal of Physical Chemistry C*, vol. 111, no. 12, pp. 4809–4814, 2007.

[2] N. Naghavi, D. Abou-Ras, N. Allsop et al., "Buffer layers and transparent conducting oxides for chalcopyrite $Cu(In,Ga)(S,Se)_2$ based thin film photovoltaics: present status and current developments," *Progress in Photovoltaics*, vol. 18, no. 6, pp. 411–433, 2010.

[3] S. K. Sarkar, J. Y. Kim, D. N. Goldstein et al., "In_2S_3 atomic layer deposition and its application as a sensitizer on TiO_2 nanotube arrays for solar energy conversion," *Journal of Physical Chemistry C*, vol. 114, no. 17, pp. 8032–8039, 2010.

[4] Y. He, D. Li, G. Xiao et al., "A new application of nanocrystal In_2S_3 in efficient degradation of organic pollutants under visible light irradiation," *Journal of Physical Chemistry C*, vol. 113, no. 13, pp. 5254–5262, 2009.

[5] C. Gao, J. Li, Z. Shan, F. Huang, and H. Shen, "Preparation and visible-light photocatalytic activity of In_2S_3/TiO_2 composite," *Materials Chemistry and Physics*, vol. 122, no. 1, pp. 183–187, 2010.

[6] S. Günes, H. Neugebauer, and N. S. Sariciftci, "Conjugated polymer-based organic solar cells," *Chemical Reviews*, vol. 107, no. 4, pp. 1324–1338, 2007.

[7] D. Deng, M. Shi, F. Chen, L. Chen, X. Jiang, and H. Chen, "Preparation and photo-induced charge transfer of the composites based on 3D structural CdS nanocrystals and MEH-PPV," *Solar Energy*, vol. 84, no. 5, pp. 771–776, 2010.

[8] B. O'Regan and M. Grätzel, "A low-cost, high-efficiency solar cell based on dye-sensitized colloidal TiO_2 films," *Nature*, vol. 353, no. 6346, pp. 737–740, 1991.

[9] M. K. Nazeeruddin, P. Péchy, T. Renouard et al., "Engineering of efficient panchromatic sensitizers for nanocrystalline TiO_2-based solar cells," *Journal of the American Chemical Society*, vol. 123, no. 8, pp. 1613–1624, 2001.

[10] K. Murakoshi, R. Kogure, Y. Wada, and S. Yanagida, "Fabrication of solid-state dye-sensitized TiO_2 solar cells combined with polypyrrole," *Solar Energy Materials and Solar Cells*, vol. 55, no. 1-2, pp. 113–125, 1998.

[11] L. Schmidt-Mende, U. Bach, R. Humphry-Baker et al., "Organic dye for highly efficient solid-state dye-sensitized solar cells," *Advanced Materials*, vol. 17, no. 7, pp. 813–815, 2005.

[12] M. Nanu, J. Schoonman, and A. Goossens, "Solar-energy conversion in $TiO_2/CuInS_2$ nanocomposites," *Advanced Functional Materials*, vol. 15, no. 1, pp. 95–100, 2005.

[13] T. T. John, M. Mathew, C. S. Kartha, K. P. Vijayakumar, T. Abe, and Y. Kashiwaba, "$CuInS_2/In_2S_3$ thin film solar cell using spray pyrolysis technique having 9.5% efficiency," *Solar Energy Materials and Solar Cells*, vol. 89, no. 1, pp. 27–36, 2005.

[14] C. W. Bates, K. F. Nelson, S. A. Raza et al., "Spray pyrolysis and heat treatment of $CuInSe_2$ for photovoltaic applications," *Thin Solid Films*, vol. 88, no. 3, pp. 279–283, 1982.

[15] M. Nanu, J. Schoonman, and A. Goossens, "Nanocomposite three-dimensional solar cells obtained by chemical spray deposition," *Nano Letters*, vol. 5, no. 9, pp. 1716–1719, 2005.

[16] S. Aukkaravittayapun, N. Wongtida, T. Kasecwatin, S. Charojrochkul, K. Unnanon, and P. Chindaudom, "Large scale F-doped SnO_2 coating on glass by spray pyrolysis," *Thin Solid Films*, vol. 496, no. 1, pp. 117–120, 2006.

[17] N. Revathi, P. Prathap, R. W. Miles, and K. T. Ramakrishna Reddy, "Annealing effect on the physical properties of evaporated In_2S_3 films," *Solar Energy Materials and Solar Cells*, vol. 94, no. 9, pp. 1487–1491, 2010.

[18] T. T. John, S. Bini, Y. Kashiwaba et al., "Characterization of spray pyrolysed indium sulfide thin films," *Semiconductor Science and Technology*, vol. 18, no. 6, pp. 491–500, 2003.

[19] N. Barreau, A. Mokrani, F. Couzinié-Devy, and J. Kessler, "Bandgap properties of the indium sulfide thin-films grown by co-evaporation," *Thin Solid Films*, vol. 517, no. 7, pp. 2316–2319, 2009.

[20] W. T. Kim and C. D. Kim, "Optical energy gaps of β-In_2S_3 thin films grown by spray pyrolysis," *Journal of Applied Physics*, vol. 60, no. 7, pp. 2631–2633, 1986.

[21] N. Barreau, "Indium sulfide and relatives in the world of photovoltaics," *Solar Energy*, vol. 83, no. 3, pp. 363–371, 2009.

[22] J. Sterner, J. Malmström, and L. Stolt, "Study on ALD In_2S_3/Cu(In, Ga)Se_2 interface formation," *Progress in Photovoltaics*, vol. 13, no. 3, pp. 179–193, 2005.

[23] K. Kambas, J. Spyridelis, and M. Balkanski, "Far infrared and raman optical study of α- and β-In_2S_3 compounds," *Physica Status Solidi*, vol. 105, no. 1, pp. 291–296, 1981.

[24] H. Tao, H. Zang, G. Dong, J. Zeng, and X. Zhao, "Raman and infrared spectroscopic study of the defect spinel $In_{21.333}S_{32}$," *Optoelectronics and Advanced Materials, Rapid Communications*, vol. 2, no. 6, pp. 356–359, 2008.

[25] M. Repková, P. Němec, and M. Frumar, "Structure and thermal properties of Ge–In–S chalcogenide glasses," *Journal of Optoelectronics and Advanced Materials*, vol. 8, no. 5, pp. 1796–1800, 2006.